AIAA SciTech
5-9 January 2015, Kissimmee, Florida
56th AIAA/ASCE/AHS/ASC Structures, Structural Dynamics, and Materials Conference

Combined Multiscale Creep Strain and Creep Rupture Modeling for Composite Materials

Eric M. Jensen[1] and Ray S. Fertig, III.[2]
Department of Mechanical Engineering, University of Wyoming, Laramie, WY, 82071

In this study, a novel multiscale combined creep strain and creep rupture model is proposed. By comparing to experimental data it was shown that the model provides accurate creep rupture predictions for unidirectional off-axis specimens. The creep strain model provides accurate predictions within the confines of the linear elastic restrictions used in its development. This creep strain and creep rupture model was incorporated into a progressive failure finite element simulation so that the effects of load redistribution could be considered, which tended to increase the life of the part. The finite element implementation also allowed for the consideration of realistic geometries resulting in complex stress states. By considering a perfectly flat specimen and one containing worst case thickness variation the experimental open hole creep rupture data was bounded. This suggests that by quantifying material defects realistic lifetime predictions can be made and an estimate of scatter can be acquired.

Nomenclature

B_i	=	static failure coefficients ($i = t, s1, s2$)
E	=	Young's modulus of matrix
E_{deg}	=	Degraded Young's modulus of matrix
h	=	Planck's constant
I_i	=	transversely isotropic matrix stress invariants ($i = t, s1, s2, h$)
k	=	Boltzmann constant
K_b	=	rate of microcracking
M	=	proportionality constant relating creep strain to microcrack density
n	=	damage variable
n_0	=	equilibration parameter that depends on damage accumulation exponent
$\mathbf{Q_m}$	=	Matrix mapping composite to matrix stress
t	=	time
t_f	=	time to failure
T	=	temperature
U	=	activation energy for creep rupture
K_b	=	pressure strengthening coefficient
β	=	pressure strengthening coefficient
γ	=	activation volume
ε	=	Matrix strain
ε_f	=	Matrix strain due at failure
ε_0	=	Matrix strain due to initial elastic loading
λ	=	shape exponent
$\boldsymbol{\sigma_c}$	=	composite stress vector
σ_{eff}	=	effective stress
$\boldsymbol{\sigma_m}$	=	matrix stress vector

---

[1] Graduate Student, Mechanical Engineering Department, Dept. 3295, 1000 E. University Ave., AIAA Student Member.
[2] Assistant Professor, Mechanical Engineering Department, Dept. 3295, 1000 E. University Ave., AIAA Member.

τ_0 = matrix shear strength

I. Introduction

FIBER reinforced polymers (FRPs) continue to be used in ever increasing quantities for large weight-critical structures, such as wind turbines and aircraft.[1, 2] These structures are designed to be in service for years or even decades and catastrophic failure can have severe consequences. Therefore, long term creep and creep rupture predictions are of critical importance. To this end, a multiscale creep strain and creep rupture model based on the kinetic theory of fracture has been developed and implemented in a progressive failure subroutine for the finite element software Abaqus.[3] This novel approach combines continuum damage mechanics for predicting creep strain with discrete damage mechanics for predicting the effects of rupture. Experimental data was collected in order to calibrate the model and open hole creep rupture data was used to test the models predictive capabilities. By considering realistic geometries accurate lifetime predictions can be achieved and insight into the scatter in time to failure of a component can be gained.

II. Model Development

The proposed creep rupture model is based on the kinetic theory of fracture, which treats damage as a thermally activated process.[4-8] Damage is predominantly accumulated in the polymer matrix constituent in the form of microcracks.[9] The rate of microcracking, K_b, can be described as

$$K_b(t) = \frac{kT}{h}\exp\left(-\frac{U-\gamma\sigma(t)}{kT}\right) \tag{1}$$

where U is the activation energy, γ is the activation volume, h is Planck's constant, k is Boltzman's constant and T is the absolute temperature. The rate of microcracking is dependent on the applied stress which, in the general case, can vary with time denoted as $\sigma(t)$. The damage evolution can then be described by a differential equation as proprosed by Fertig and Kenik,[10, 11] which is an enhancement of that proposed by Hansen and Baker-Jarvis[12] and Hsiao et al.[13] as

$$\frac{dn}{dt} = \left(n_0 - n\right)^{\lambda} K_b \tag{2}$$

The scalar damage parameter, n, represents the ratio of the current microcrack density to the microcrack density at failure ($n(t=0)=0$ *and* $n(t_f)=1$), t is time and λ is an exponential shape factor. The constant n_o is determined by forcing

$$\int_0^1 \frac{dn}{\left(n_0 - n\right)^{\lambda}} = 1 \tag{3}$$

which forces the differential equation to reproduce Zhurkov's durability equation[4] for the application of a constant stress. Solving the differential equation leads to two forms of the damage evolution as

$$n(t) = \begin{cases} n_0\left(1-\exp\left\{-\dfrac{kT}{h}\exp\left(\dfrac{-U}{kT}\right)\displaystyle\int_0^t \exp\left(\dfrac{\gamma\sigma(\tau)}{kT}\right)d\tau\right\}\right), & \lambda = 1 \\ n_0 - \left\{n_0^{(1-\lambda)} - (1-\lambda)\dfrac{kT}{h}\exp\left(\dfrac{-U}{kT}\right)\displaystyle\int_0^t \exp\left(\dfrac{\gamma\sigma(\tau)}{kT}\right)d\tau\right\}^{\frac{1}{1-\lambda}}, & \lambda \neq 1 \end{cases} \tag{4}$$

This formulation allows for the damage evolution to be predicted for an arbitrary time varying stress. An arbitrary time varying stress can be approximated by constant stress time intervals. Then the total damage accumulation at some time t after a previous time t_i can be calculated assuming a constant stress, σ_s, for the time interval $(t-t_i)$ as

$$n(t) = \begin{cases} \left(n_0 - (n_0 - n_i)\exp\left\{-\dfrac{kT}{h}\exp\left(-\dfrac{U-\gamma\sigma_s}{kT}\right)\left[t-t_i\right]\right\}\right), & \lambda = 1 \\ n_0 - \left\{\left(n_0 - n_i\right)^{(1-\lambda)} - (1-\lambda)\dfrac{kT}{h}\exp\left(-\dfrac{U-\gamma\sigma_s}{kT}\right)\left[t-t_i\right]\right\}^{\frac{1}{1-\lambda}}, & \lambda \neq 1 \end{cases} \tag{5}$$

The n_i parameter is the normalized damage state at time t_i. This formulation lends itself to implementation in a finite element analysis where time is incremented discretely and the stress is assumed to remain constant for the time increment. For a constant applied stress the time to failure can be found as,

$$t_f = \frac{h}{kT}\exp\left(\frac{U - \gamma\sigma_s}{kT}\right) \tag{6}$$

The above formulation requires a scalar stress measure, so an effective stress is proposed. Since the damage being modeled is microcracking in the polymer matrix material the stress state in the matrix is the quantity of interest. A mapping $\mathbf{Q_m}$ exists which maps the composite stress state to volume averaged matrix stress state as[14-17]

$$\boldsymbol{\sigma}_\mathbf{m} = \mathbf{Q_m}\boldsymbol{\sigma}_\mathbf{c} \tag{7}$$

where $\boldsymbol{\sigma}_\mathbf{m}$ is the matrix stress tensor and $\boldsymbol{\sigma}_\mathbf{c}$ is the composite stress tensor. Then an effective matrix stress as proposed by Fertig[18] can be calculated as

$$\sigma_{eff} = \sqrt{\frac{B_t}{B_{s1}}\{I_t\}^2 + \frac{1}{\left(1 - \frac{\beta}{\tau_0}\{-I_h\}\right)}\left[I_{s1} + \frac{B_{s2}}{B_{s1}}I_{s2}\right]} \tag{8}$$

where τ_o is the matrix shear strength, β is a pressure strengthening term, B_t, B_{s1}, B_{s2} are failure coefficients determined from transverse tension, transverse compression, and in plane shear respectively. The $\{\ \}$ denote Macaulay brackets such that if the quantity inside is negative the quantity is zero and if the quantity inside the brackets is positive it remains that quantity. The I_t, I_{s1}, I_{s2}, and I_h terms are transversely isotropic stress invariants

$$\begin{aligned}
I_t &= \frac{\sigma_{22} + \sigma_{33} + \sqrt{(\sigma_{22} + \sigma_{33})^2 - 4(\sigma_{22}\sigma_{33} - \sigma_{23})}}{2} \\
I_{s1} &= \sigma_{12}^2 + \sigma_{13}^2 \\
I_{s2} &= \frac{1}{4}(\sigma_{22} - \sigma_{33})^2 + \sigma_{23}^2 \\
I_h &= \sigma_{22} + \sigma_{33}
\end{aligned} \tag{9}$$

Static failure of the matrix constituent can be predicted with the related Fertig Failure Criterion[18] as

$$B_t\{I_t\}^2 + \frac{1}{\left(1 + \frac{\beta}{\tau_0}\{-I_h\}\right)}\left[B_{s1}I_{s1} + B_{s2}Is2\right] = 1 \tag{10}$$

With this formulation the time to failure of a composite laminate can be predicted for an arbitrary stress history. However, there is no information about the deformation. In many cases the function of a structural component limits deformation. Therefore, it is important that creep deformation is also considered. Zhurkov and Kuksenko[9] showed that in a polymer the creep deformation is linearly related to microcrack density and proposed a form as

$$\varepsilon = \varepsilon_0 + \varepsilon_m N \tag{11}$$

where ε is the strain in the loading direction, ε_0 is the initial strain state prior to damage, ε_m is a proportionality constant, and N is the microcrack density. Changing the microcrack density variable, N, to a normalized microcrack density, n, results in an equivalent relationship

$$\varepsilon = \varepsilon_0 + Mn \tag{12}$$

where M is the new proportionality constant relating change in strain to a normalized microcrack density. If it is assumed that the initial state is undamaged and that the initial strain is linear elastic then

$$\varepsilon_0 = \varepsilon_{elastic} = \frac{\sigma_a}{E} \tag{13}$$

where E is the elastic modulus of the material and σ_a is the applied stress. The normalized damage parameter is unity at failure so the proportionality constant is simply

$$M = \varepsilon_f - \varepsilon_0 \tag{14}$$

where ε_f is the strain at failure. Fiber reinforced polymers tend to fail in a rather brittle and catastrophic manner. Therefore, as a first order approximation it is assumed that the material behaves linear elastically to failure then

$$\varepsilon_f = \frac{\sigma_{UT}}{E} \tag{15}$$

where σ_{UT} is the ultimate tensile strength of the material.

In order to implement this methodology in a finite element analysis where stresses are typically calculated from strains based on a stiffness matrix it is desirable to formulate this as stiffness degradation. Therefore, an effective modulus, E_{deg}, can be defined as,

$$E_{\text{deg}} = \frac{\sigma_a}{\varepsilon} \tag{16}$$

Substituting this into the strain relationship results in

$$\frac{E_{\text{deg}}}{E} = \frac{\sigma_a}{\sigma_a + \left(\sigma_{UT} - \sigma_a\right)n} \tag{17}$$

Until this point the strain description has been based on the one dimensional case for a polymer under tensile load. However, stress and strain are tensors and the polymer matrix in the composite will be subjected to complex stress states. Therefore, an effective stress measure is needed. The same effective stress as described above is used resulting in a description for the modulus degradation as

$$\frac{E_{\text{deg}}}{E} = \frac{\sigma_{eff}^{a}}{\sigma_{eff}^{a} + \left(\sigma_{eff}^{UT} - \sigma_{eff}^{a}\right)n} \tag{18}$$

Poisson's ratio is held constant during the analysis.

III. Finite Element Implementation

The creep rupture and creep strain model described above have been combined with a static failure criterion and implemented in a progressive failure user material subroutine (UMAT) for the finite element software Abaqus. Although the model can handle an arbitrary stress history the focus of this study is the prediction of deformation and failure under a constant load. In order to do this the subroutine breaks the analysis into a load step and a hold load step.

During the load step a prescribed load is applied to the modeled geometry and the stress state is calculated assuming linear elasticity. Then, mapping the composite stress state to a volume average matrix and fiber stress state, static failure of the individual constituents is evaluated. Matrix failure is predicted by the Fertig failure criterion and fiber failure is predicted by a maximum fiber stress criterion. If matrix failure is predicted, then the composite stiffness tensor is degraded to be that predicted by a hexagonal micromechanics model with the matrix moduli decreased to 1% of the original values. If fiber failure is predicted, then composite stiffness is degraded to that predicted by a hexagonal micromechanics model with both the matrix and fiber moduli degraded to 1% of the original values. For this estimate it was assumed that no change in the constituent Poisson's ratios occurs. This process is iterated until a converged solution is reached. All of the material properties, including the degraded stiffness matrices, are provided by the user in a material text file. This allows for alternative material degradation methods to be investigated in the future.

Once a converged solution is achieved in the load step the hold load step begins. This step is broken into a predetermined number of time increments. The stress is calculated based on the stiffness at the end of the previous increment. It is assumed that the stress state remains constant for the duration of the time increment. If the element did not fail previously then damage accumulation for the increment is calculated based on Equation (5). The effective modulus of the matrix material at the end of the increment is calculated based on Equation (18). The effects of this matrix degradation on the composite properties are estimated by linear least squares regressions to the composite properties predicted by a hexagonal micromechanics model with varying matrix moduli which have been shifted to ensure that the original properties are reproduced when no damage has occurred. The relationships are,

$$
\begin{aligned}
E_{c2} = E_{c3} &= \left(0.7273\frac{E_{m\deg}}{E_m} + 0.2727\right)E_{c2} \\
\nu_{c23} &= \left(-0.078\frac{E_{m\deg}}{E_m} + 1.078\right)\nu_{c23} \\
G_{c12} = G_{c13} &= \left(0.9013\frac{E_{m\deg}}{E_m} + 0.0987\right)G_{c12} \\
G_{c23} &= \frac{E_{c2}}{2\left(1+\nu_{c23}\right)}
\end{aligned}
\tag{19}
$$

The other material parameters are not significantly affected by small changes in matrix modulus so they were held constant. The degraded stiffness tensor is stored and is used to predict the starting stress and strain point in the next increment. If creep rupture is predicted then the composite properties are discretely degraded to those of the static matrix failed state.

IV. Model Calibration

A complete material characterization was performed on unidirectional pre-impregnated carbon/epoxy (Zoltek Panex 35 carbon fiber/Hexcel M9.7 Epoxy resin) material system. Strain was measured using foil resistance strain gages and an in house digital image correlation (DIC) system.[19] The DIC technique also allows for the measurement of two dimensional strain fields on the surface of the specimens. Tension and compressions tests were performed according to ASTM D3039 and ASTM D3410.[20, 21] Shear properties were extracted using the v-notch beam tests of ASTM D5379.[22] The extracted elastic material properties are summarized in Table 1 and the measured strengths are summarized in Table 2.

Table 1. Summary of measured elastic material properties

	E_1 (GPa)	E_2 (GPa)	G_{12}(GPa)	G_{23}(GPa)	ν_{12}	ν_{23}
Average	134	8.91	4.04	2.65	0.326	0.554
Std Dev	9.03	0.658	0.464	0.316	0.039	0.089
COV	0.067	0.074	0.115	0.119	0.120	0.161

Table 2. Summary of measured composite strengths

	S_{11}^{UT} (MPa)	S_{11}^{UC} (MPa)	S_{22}^{UT} (MPa)	S_{22}^{UC}(MPa)	S_{12}^{US}(MPa)	S_{23}^{US}(MPa)
Average	1933	832	45.1	147	57.2	32.4
Std Dev	52.8	74.3	2.56	2.95	3.87	6.18
COV	0.027	0.089	0.057	0.020	0.068	0.191

Although this is a complete set of composite properties, the material properties of the individual constituents must also be known, as the proposed methodology is a multiscale approach. Unfortunately, the manufacturers do not provide all of the necessary material properties. Furthermore, there is much difficulty associated with predicting composite material properties. So a complete set of consistent composite and constituent material properties were estimated using the Autodesk Simulation Composite Analysis 2014 Material Manager.[23] The results are provided in Table 3. This consistent set of composite and constituent material properties were used in all subsequent analyses. These material properties produce a matrix stress mapping of

$$
Q_m = \begin{bmatrix}
0.0274336 & 0.399300 & 0.399300 & 0.000000 & 0.000000 & 0.000000 \\
0.0015567 & 0.833861 & 0.137345 & 0.000000 & 0.000000 & 0.000000 \\
0.0015567 & 0.137345 & 0.833861 & 0.000000 & 0.000000 & 0.000000 \\
0.000000 & 0.000000 & 0.000000 & 0.658906 & 0.000000 & 0.000000 \\
0.000000 & 0.000000 & 0.000000 & 0.000000 & 0.658906 & 0.000000 \\
0.000000 & 0.000000 & 0.000000 & 0.000000 & 0.000000 & 0.696516
\end{bmatrix}
\tag{20}
$$

The matrix shear strength, τ_0, was estimated to be the volume average matrix shear stress at composite failure. The pressure strengthening term was taken to be similar to published values.[18, 24] From the measured transverse tensile strength, compressive strength and in plane shear strength the failure coefficients of the Fertig failure criterion were calculated. These values are summarized in Table 4.

The activation energy and activation volume, U and γ, of the material were determined by fitting to experimental creep rupture data of 90° and 45° off axis specimens. The shape parameter, λ, was determined by forcing the creep strain predictions to follow a similar form to experimental creep strain results.[9] The results are summarized in Table 4. With these parameters, the model is calibrated and creep strain and creep rupture predictions can be made.

Table 3. Consistent micromechanics material properties

	Matrix	Fiber	Composite
E_1 (GPa)	3.491	224.8	133.9
E_2 (GPa)	3.491	17.34	9.040
G_{12}(GPa)	1.229	18.20	3.848
G_{23}(GPa)	1.229	6.618	2.939
ν_{12}	0.42	0.271	0.330
ν_{23}	0.42	0.310	0.538

Table 4. Summary of extracted failure coefficients and creep constants

τ_0 (MPa)	β	B_{s1} (MPa^{-2})	B_{s2} (MPa^{-2})	B_t (MPa^{-2})	U (kJ/mol)	γ (kJ/MPAmol)	λ
37.7	0.35	7.0398e-4	8.729e-4	5.5230e-4	259.1	4.82	9

V. Results

After the model calibration was complete, comparisons to experimental data were needed to validate that the model was functioning properly. The creep predictions based on the analytic time to failure of 90° and 45° off axis specimens are compared with experimental data in Figure 1. It can be seen that the model accurately predicts creep rupture of the unidirectional FRPs. However, this is the same experimental data that was used to extract the activation energy and activation volume, so a good fit is expected. In order to test the predictive capabilities of the model analytic time to failure predictions of open hole specimens were made based on an approximate maximum stress at the edge of the hole using a stress concentration factor of 2. A comparison to experimental data is shown in Figure 2. The analytic prediction does pass through the range of experimental data but it is clear that the behavior is not as well described as the whole off-axis tests. In fact, the experimental open hole data seems to be following a much more vertical path than the whole specimens suggesting that another factor may be influencing failure of the open hole specimens.

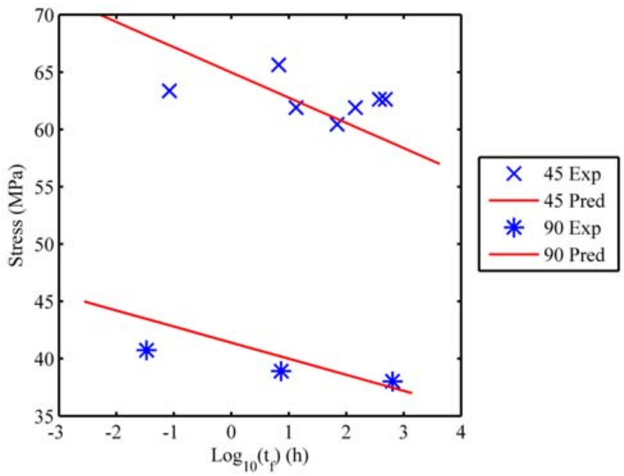

Figure 1. Comparison of experimental creep rupture and model predictions.

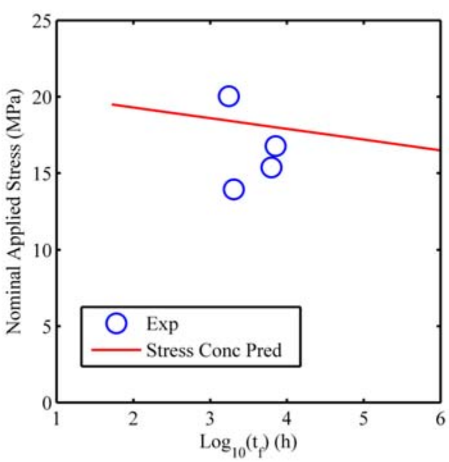

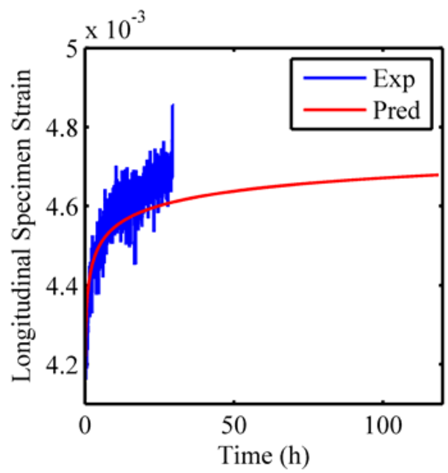

(Left) Figure 2. Open hole creep rupture experiments and analytical predition comparison.
(Right) Figure 3. 90° creep strain comparison with same initial strain.

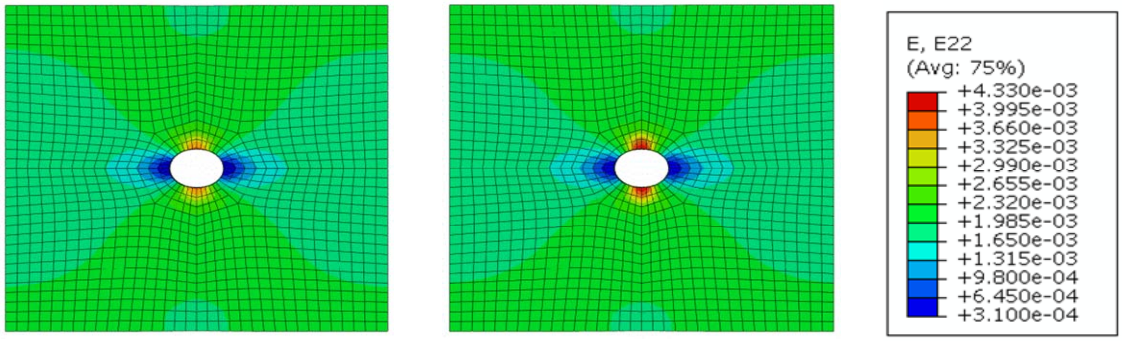

(a) (b)

Figure 4. Creep strain evolution of open hole specimen (a) initial state and (b) after 10^{10}s.

A comparison of the creep strain prediction to experimental creep strain for a 90° off-axis specimen, with the same initial strain point based on the elastic modulus of the composite, is shown in Figure 3. The shape of the predicted creep strain curve and the experimental measurement are very similar suggesting that the shape parameter of 9 is a reasonable choice. Furthermore, the amount of creep strain predicted is very similar to what was measured. The total strain of the 45° off-axis specimens was significantly under-predicted but the 45° off-axis specimens exhibited non-linear behavior that this model is not currently capable of considering. Within the limitations of the assumptions used in its derivation the strain model appears to be providing accurate predictions.

The finite element implementation of the combined creep strain and creep rupture model allowed for the effect of load redistribution due to creep strain on the time to failure to be investigated. Simulations were performed on perfectly flat open hole specimens and the creep strain localized at the edge of the hole as expected. This is shown in Figure 4. Time to failure predictions, based on the initial nominal stress and progressive failure, for three load cases are provided in Table 5. Clearly the load redistribution tends to increase the time to failure of the component. This suggests that by neglecting load redistribution overly conservative failure predictions could be made. The finite element predictions are provided as the red curves in Figure 5. Clearly, these over-predict the life of the open hole specimens and still do not capture the trend. Another factor must be influencing the experimental failure times.

Table 5. Flat open hole FEA time-to-failure predictions

Load (N)	Nominal Stress (MPa)	t_f Prediction (s)	t_f Progressive Prediction (s)
1000	18.0	3.80e10	1.11e13
1111	20.0	1.19e8	1.01e10
1200	21.6	1.18e6	2.11e7

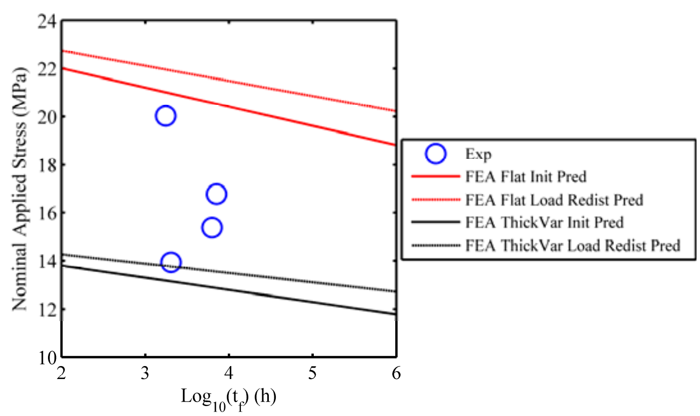

Figure 5. Comparison of FEA open hold time-to-failure and experimental data points.

Previously, it has been shown that thickness variation exists in laminates such as the ones used for this study.[19] This thickness variation leads to stress and strain inhomogeneity in the composite. This strain inhomogeneity is exacerbated by creep deformation as illustrated by the two dimensional strain field measurements in Figure 6. It is possible that the open hole stress concentration is interacting with stress concentrations due to thickness variation resulting in the unusual vertical nature of the experimental data. In order to investigate this, creep failure simulations on an open hole composite containing measured thickness variation was performed. This measured thickness variation likely represents a worst case

Table 6. Open hole FEA with thickness variations time-to-failure predictions

Load (N)	Nominal Stress (MPa)	t_f Prediction (s)	t_f Progressive Prediction (s)
750	13.5	1.38e6	4.11e7
800	14.4	2.20e4	9.90e4
850	15.3	3.52e2	1.00e3

scenario as steps were taken to minimize this in future samples used for the open hole tests. The addition of the thickness variation dramatically reduced the time to failure and load carrying capacity of the open hole specimen and failure predictions for three load states are provided in Table 6. Again, longer life was predicted by considering load redistribution. When these predictions are compared to the experimental data in Figure 5, the failure predictions with worse case thickness variation fall below the experimental data points. By considering a perfectly flat specimen and one with worst case thickness variation the open hole creep data was bounded. This illustrates that by quantifying and considering material defects this methodology allows for realistic life predictions to be made on geometries resulting in complex stress states.

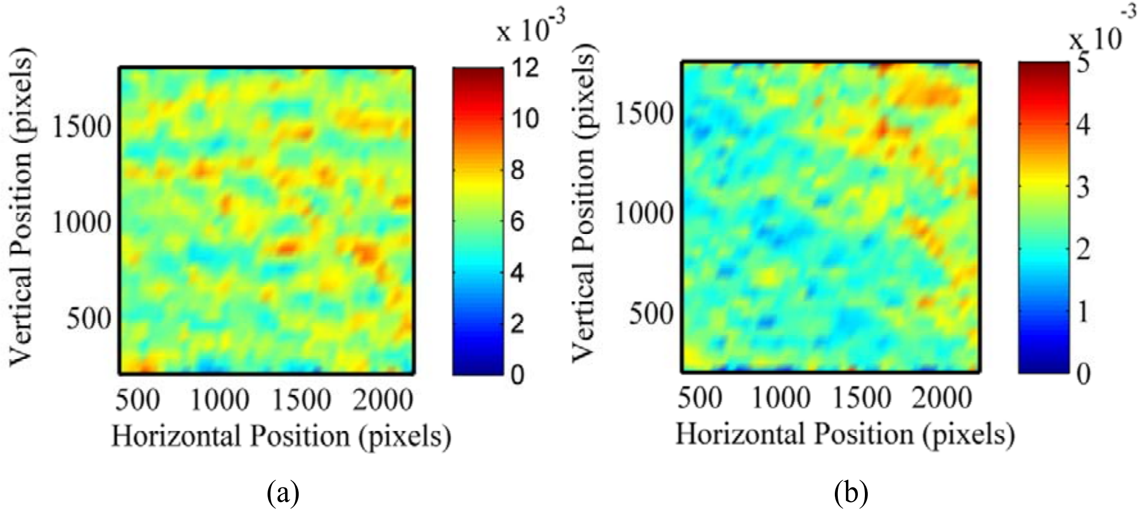

Figure 6. 45° specimen strain localization (a) elastic and (b) creep.

VI. Conclusion

This study proposed a novel multiscale combined creep strain and creep rupture model. By comparing to experimental data it was shown that the model provides accurate creep rupture predictions for unidirectional off-axis specimens. The creep strain model provides accurate predictions within the confines of the linear elastic restrictions used in its development. By incorporating this creep strain and creep rupture model in a progressive failure finite element simulation the effects of load redistribution can be considered, which tends to increase the life of the part. The finite element implementation also allows for the consideration of realistic geometries resulting in complex stress states. By considering a perfectly flat specimen and one containing worst case thickness variation the experimental open hole creep rupture data was bounded. This suggests that by quantifying material defects realistic lifetime predictions can be made and an estimate of scatter can be acquired. This may lead to more accurate and reliable failure predictions of critical structures in the future.

Acknowledgments

Funding for this work is gratefully acknowledged from the Wyoming NASA Space Grant Consortium, NASA Grant #NNX10A095H, and the University of Wyoming’s College of Engineering and Applied Sciences Energy Graduate Assistantship.

References

The following pages are intended to provide examples of the different reference types, as used in the AIAA Style Guide.

[1] Soutis, C. "Fibre reinforced composites in aircraft construction," *Progress in Aerospace Sciences* Vol. 41, No. 2, 2005, pp. 143-151. doi: http://dx.doi.org/10.1016/j.paerosci.2005.02.004

[2] Brøndsted, P., Lilholt, H., and Lystrup, A. "COMPOSITE MATERIALS FOR WIND POWER TURBINE BLADES," *Annual Review of Materials Research* Vol. 35, No. 1, 2005, pp. 505-538. doi: 10.1146/annurev.matsci.35.100303.110641

[3] SIMULIA. "Abaqus." 6.11 ed., Dassault Systemes, 2011.

[4] Zhurkov, S. N. "Kinetic Concept of the Strength of Solids," *International Journal of Fracture* Vol. 1, 1965, pp. 311-323.
[5] Coleman, B. D. "Time dependence of mechanical breakdown phenomena," *Journal of Applied Physics* Vol. 27, No. 8, 1956, pp. 862-866.
[6] Regel, V. R. "Kinetic theory of strength as a scientific basis for predicting the lifetime of polymers under load," *Mechanics of Composite Materials* Vol. 7, No. 1, 1971, pp. 82-93.
[7] Regel, V. R., Leksovskii, A. M., Slutsker, A. I., and Tamuzh, V. P. "Polymer breakdown and fatigue," *Mechanics of Composite Materials* Vol. 8, No. 4, 1972, pp. 516-527.
[8] Tomashevskii, E. E., Zakrevskii, V. A., Novak, I. I., Korsukov, V. E., Regel, V. R., Pozdnyakov, O. F., Slutsker, A. I., and Kuksenko, V. S. "Kinetic micromechanics of polymer fracture," *International Journal of Fracture* Vol. 11, No. 5, 1975, pp. 803-815.
[9] Zhurkov, S. N., and Kuksenko, V. S. "The micromechanics of polymer fracture," *International Journal of Fracture* Vol. 11, No. 4, 1975, pp. 629-639.
[10] Fertig III, R. S., and Kenik, D. J. "Predicting Composite Fatigue Life Using Constituent-Level Physics," *52nd AIAA/ASME/ASCE/AHS/ASC Structures, Structural Dynamics and Materials Conference*. AIAA, Denver, CO, 2011, pp. 11-11.
[11] Fertig III, R. S., and Kenik, D. J. "Physics-Based Fatigue Life Prediction of Composite Structures," *NAFEMS World Congress 2011*. Vol. CD-ROM, NAFEMS, Boston, MA, 2011, p. 12.
[12] Hansen, A. C., and Baker-Jarvis, J. "A rate dependent kinetic theory of fracture for polymers," *International Journal of Fracture* Vol. 44, 1990, pp. 221-231.
[13] Hsiao, C. C., Moghe, S. R., and von Schmeling, H. H. K. "Time-Dependent Mechanical Strength of Oriented Media," *Journal of Applied Physics* Vol. 39, No. 8, 1968, pp. 3857-3861.
[14] Fertig III, R. S. "A computationally efficient method for multiscale modeling of composite materials: Extending multicontinuum theory to complex 3D composites," *SAMPE 2010 Fall Technical Conference*. SAMPE, Salt Lake City, UT, 2010, pp. 11-11.
[15] Fertig III, R. S. "An accurate and efficient method for constituent-based progressive failure modeling of a woven composite," *TMS 2010 Annual Meeting*. Vol. 2, TMS, Seattle, WA, 2010, pp. 223-230.
[16] Dvorak, G. J. "On Uniform Fields in Heterogeneous Media," *Proceedings of the Royal Society of London. Series A: Mathematical and Physical Sciences* Vol. 431, No. 1881, 1990, pp. 89-110.
[17] Dvorak, G. J., and Benveniste, Y. "On Transformation Strains and Uniform Fields in Multiphase Elastic Media," *Proceedings of the Royal Society of London. Series A: Mathematical and Physical Sciences* Vol. 437, No. 1900, 1992, pp. 291-310.
[18] Fertig III, R. S. "Bridging the gap between physics and large-scale structural analysis: a novel method for fatigue life prediction of composites," *SAMPE 2009 Fall Technical Conference*. Wichita, KS, 2009.
[19] Jensen, E. M., Leonhardt, D. A., and Fertig III, R. S. "Effects of thickness and fiber volume fraction variations on strain field inhomogeneity," *Composites Part A: Applied Science and Manufacturing* Vol. 69, No. 0, 2015, pp. 178-185. doi: http://dx.doi.org/10.1016/j.compositesa.2014.11.019
[20] ASTM. "Standard Test Method for Tensile Properties of Polymer Matrix Composite Materials," *ASTM D3039*. ASTM International, 2008.
[21] ASTM. "Standard Test Method for compressive Properties of Polymer Matrx Composite Materials with Unsupported Gage Section by Shear Loading," *ASTM D3410*. ASTM International, 2003.
[22] ASTM. "Standard Test Method for Shear Properties of Composite Materials by the V-Notched Beam Method," *ASTM D5379*. ASTM International, 2005.
[23] Autodesk. "Autodesk Simulation Composite Analysis 2014." 2014 ed., Autodesk, Inc., 2014.
[24] Hoppel, C. P. R., Bogetti, T. A., and Gillespie, J. W. "Literature Review-Effects of hydrostatic pressure on the mechanical behavior of composite materials," *Journal of Thermoplastic Composite Materials* Vol. 8, 1995, pp. 375-409.